

Bio-Inspired Robotics: Kinematic and Gait Analysis of Quad and Hexa-Legged Systems

Spoorthi Singh¹, Mohammad Zuber², Naman Bhat³, Rathina Kumar.S⁴, Ernie Illyani Basri⁵, Kamarul Arifin Ahmad⁶, Manish Varun Yadav⁷, Navya Thirumaleshwar Hegde^{8*}

^{1,3,4} Department of Mechatronics, Manipal Institute of Technology, Manipal Academy of Higher Education, Manipal, India
^{2,7,8} Department of Aeronautical and Automobile Engineering, Manipal Institute of Technology, Manipal Academy of Higher Education, Manipal, India

^{5,6} Department of Aerospace Engineering, Faculty of Engineering, Univesiti Putra Malaysia, UPM Serdang, Selangor, Malaysia, 43400

Email: ¹ spoorthi.shekar@manipal.edu, ² mohammad.zuber@manipal.edu, ³ naman.bhat@learner.manipal.edu, ⁴ rathinakumar.subramanian@learner.manipal.edu, ⁵ ernebasri@gmail.com, ⁶ aekamarul@upm.edu.my, ⁷ yadav.manish@manipal.edu, ⁸ navya.hegde@manipal.edu

*Corresponding Author

Abstract—Navigating hazardous environments, such as areas with fire risks, wild animal activity, or inaccessible terrains, poses significant challenges, necessitating the development of bio-inspired robotic systems. This study focuses on the biomechanical design and kinematic analysis of a spider-mimicking robot, specifically examining quad and hexa-legged configurations to optimize movement efficiency and stability. The research employed 3D Computer-Aided Design (CAD) in Fusion 360 to model and simulate the robot's leg framework, analyzing deformation, tension, and strain. Fused Deposition Modelling (FDM) with Poly Lactic Acid (PLA) material was used for component fabrication, chosen for its balance of lightweight properties and structural integrity, validated through stress analysis. A single limb's forward and reverse kinematics were studied, enabling the development of optimized gait patterns. SIMSCAPE Multibody in MATLAB was utilized for dynamic simulations, and Proportional Derivative (PD) and Proportional Integral Derivative (PID) controllers were tested to evaluate trajectory tracking accuracy and stability. Results show that the six-legged configuration exhibits superior stability with a 15% improvement in gait cycle efficiency and a 20% reduction in energy consumption per stride compared to the four-legged counterpart. The use of PID controllers further enhanced performance, achieving a 12% improvement in settling time and reducing oscillations in trajectory tracking tasks. The choice of PLA material ensured durability under operational loads, with minimal deformation over repeated stress cycles. Servomotor selection and configuration were tailored to optimize torque and speed, enabling precise leg control. This study highlights the potential of bio-inspired robots to advance robotic mobility through optimized kinematics and material choices.

Keywords—Bio-Inspired Robot; Forward and Reverse Kinematics; Hexa Leg Robot; Limb Kinematics; Quad Leg Robot; Spider-Mimicking Robot.

I. INTRODUCTION

Over the past two decades, technological advancements have addressed human safety concerns, especially in hazardous environments. Robotics, inspired by animal behavior, have been developed for tasks like animal welfare and navigating difficult, dangerous terrains without causing disruption. Spider robots, as a subset of legged robotic systems, play a pivotal role in advancing robotics technology,

offering unique advantages in navigation and adaptability across complex terrains. Their biomimetic design allows for enhanced mobility in environments where traditional wheeled robots falter, making them invaluable for applications in search and rescue, exploration, and hazardous material handling. The spider robot [1]-[6], that uses multiple gaits for the movements depending on the variation of speed of the bot. The spider robot is a six- or eight-legged robot which mimics the motion of a spider. The present-day spider robots that exist generally consist of 12 to 24 motors, resulting in 12 to 24 Degrees of Freedom (DOF). Spider robot projects have multiple levels of complexity. Six- to eight- legged robots, although more complex in design and fabrication, have the advantages of better mobility and weight balance over four-legged robots. Spider robots existing are also grouped into autonomous and non-autonomous robots. Spider pig (Linkoping University) is an example of an autonomous robot. Such robots use image processing techniques and artificial intelligence to plan paths and carry out specific functions. Non-autonomous robots are simpler robots which are controlled by human input and monitoring. Autonomous robots can operate independently, making decisions based on their programming, sensors, and AI without direct human control. They can perceive their environment, process information, and perform tasks with minimal or no human input. Examples include self-driving cars, robotic vacuum cleaners, and industrial robots in smart manufacturing.

Non-autonomous robots rely heavily on human control, either through direct input (like remote control) or pre-programmed instructions. They do not have the capability to adapt or make decisions based on environmental changes. Examples include remote-controlled drones, simple industrial machines, and tele-operated robots. Wall climbing robots are spider bots which are being used to climb on vertical walls to perform various tasks. Spider robots can climb walls by means of multiple different methods such as pneumatic actuation, magnetic adhesion, propellor, rope or rail gripping, and bio-inspired adhesion [7]-[8].

RHex Robotic Hexapod [9] uses one motor for each leg, therefore giving it only one degree of freedom. The leg rotates in half a circle to cause motion. This robot has been less complex in design and maintenance. It shows great



performance in stair climbing and uneven surface conditions. Lauron III [10], can traverse over uneven land easily, having six legs and three degrees of freedom for each limb. To make it autonomous, the robot was enabled with current sensors, infrared proximity sensors, and inclinometers. Each foot was equipped with a three-axis force sensor. Szabad(ka) [11] robot is an example of a robot that was made on a tight budget. The weight of the robot was roughly 10 kg and was made of aluminium. The height is roughly 300mm. This robot used a gearbox to provide different gear ratios. Hexapods can be separated into different designs based on the shape of their legs and body. The difference in performance of the shape of legs would be seen in different terrains that the robot traverses. Legs can be shaped as fishhooks, flat columns or even wheels can be used. Wheels would obviously have the best mobility on flat surfaces and poor mobility on rocky terrains. Fishhooks would be able to traverse sloping and rocky terrains easily but are susceptible to poor performance on flat surfaces [12]-[16]. Flat columns would have an average performance on both surfaces. The shape of the body determines the overall symmetry of the robot which is important for weight balance. The body shape must be chosen while considering the design of the legs to ensure the stability of the robot. The body must also be designed such that it can accommodate all the components of the robot within itself [17]-[19].

Since authors are trying to create a mechanism for spider robots, the challenge lies in keeping its design simple as is feasible. By validating its needs for six or four legs, and if it is delivering the appropriate degree of movability with four legs, subsequently in the six-legged design, the possibility of adding a set of robotic arms to use it for obstacle avoidance through pick-and-place operations can be investigated. Hence the design discussed in this paper aims to reduce the complexity of two motors and two links from the design [20]-[22]. By removing two links from opposite sides whose range of motion is relatively less, we can achieve this. In this paper, the comprehensive design procedure with kinematic calculations and simulation analysis for leg movement is described. The more dynamic measurements performed for its trajectory of movement and control via Proportional Integral Derivative (PID) are well illustrated [23]-[27]. The configuration of a structure with a circuit diagram is investigated for the combinations of four and six legs using a model coupled to a servomotor and controlled in simulation and real-time as well. The 3D (dimension) printed fabrication has now been built to accommodate the options of six legs; however, only four legs are being attached, leaving space for either two arms or space for two more legs [28]-[32].

This paper focuses on understanding and replicating the intricate mechanics of animal locomotion. By examining the leg postures, joint angles, and movement patterns of quadrupeds like dogs and hexapods like insects, researchers aim to optimize stability, efficiency, and adaptability in robotic movement [33]-[38]. This analysis includes evaluating different gaits, such as walking, trotting, and creeping, and how these affect the robots' stability and energy consumption. The insights gained from these studies are crucial for improving the design and control algorithms of legged robots, enabling them to navigate complex terrains with greater agility and resilience [39]-[44].

This research is vital for addressing the challenge of identifying hazardous situations, such as explosions, fires, and wild animal activity, in areas that are difficult for humans to

reach. A bio-inspired spider-mimicking robot offers an effective solution, capable of navigating uneven terrain with stability and efficiency. The study focuses on optimizing the leg framework, as the number of legs directly impacts the robot's movement rate and balance. By minimizing design and circuit complexity, the research aims to create a compact, efficient robot using kinematic analysis and 3D CAD design.

Recent advancements in legged robotics focus on optimizing gaits and improving stability for hexapod and quadruped robots navigating complex terrains [63]-[67]. Gait optimization frameworks, impulse-based analysis, and reinforcement learning have been used to enhance robot locomotion and adaptability. Studies also emphasize the importance of symmetry-breaking in gait design and real-time posture control for uneven terrain navigation [68]-[70]. Additionally, bio-inspired control systems, like neural coupled pattern generators, have been implemented to ensure smooth gait transitions and robust movement [70]-[73].

Recent research also focuses on high-dynamic locomotion and fault-tolerant gaits, further improving the efficiency and reliability of multi-legged robots [74]-[76]. These developments aim to make robots more autonomous, stable, and capable of overcoming obstacles in diverse environments [76]-[80].

The paper presents a novel spider robot design emphasizing simplicity, efficiency, and cost-effectiveness. It introduces a 4+2 leg configuration, reducing motor and link complexity while maintaining stability. The robot integrates space for robotic arms, enabling both locomotion and manipulation tasks. Lightweight Poly Lactic Acid (PLA) material and 3D printing optimize weight and manufacturing cost. Advanced kinematic analysis, PID controllers, and simulation validate its application for hazardous environment navigation.

In the rest of the paper, section II discusses the mechanical design, section III presents the modelling and simulation of leg joints in SIMSCAPE multibody. Section IV covers the hardware implementation of Spiderbot. The conclusion is stated in Section V.

II. MECHANICAL DESIGN OF PROPOSED SPIDERBOT

The earlier hexabots, constructed from metals, were typically larger and heavier. In the proposed model, the authors aimed to minimize the robot's size and weight by using PLA. Authors have opted for 3D printing as the manufacturing method because it is simpler and doesn't require continuous monitoring. PLA was chosen due to its high heating resistance and rigidity, making it suitable for this application. The design for 3D printing was created using Autodesk Fusion 360.

A. Components of Proposed Spiderbot

The body of the Spiderbot including the legs and the holders are made using 3D printing technology. The robot's body was designed in fusion 360 software as shown in Fig. 1. The design includes the legs, the main body, and the snap-on fasteners. The robot was made by using two separate materials. The legs were made from a material known as Polyethylene Terephthalate Glycol (PETG), whereas the body was made from Polylactic Acid (PLA).

The Arduino and ESP8266 were programmed using the Arduino Integrated Development Environment (IDE). The components used are illustrated in Fig. 2 and briefly described.

The assembled leg design, including its isometric, side, and top views, is displayed in Fig. 3.

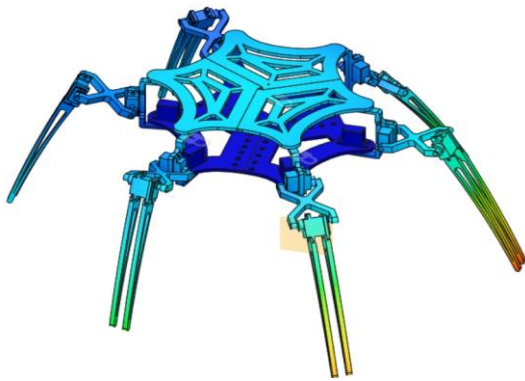


Fig. 1. Proposed Spiderbot design

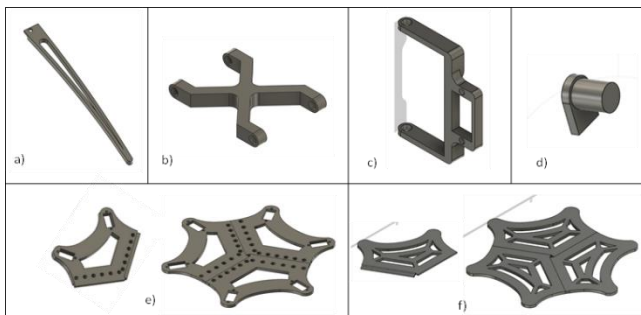


Fig. 2. Individual part design using CAD, a) Leg end, b) Middle link, c) Base link, d) Connector, e) Base plate, f) Top plate



Fig. 3. Assembled leg design with isometric side and top view

Leg end: The leg end link is the part of the robot, which encounters the ground. This part is roughly 16 cm long and 1.4 cm broad with a thickness of 5mm. The leg is joined to a motor with the help of screws which are joined to the rest of the body.

Middle link: This link connects the leg end to the rest of the body. It has two motors fixed onto it. The holes made in the end are for the rotors of the two motors to fit. This part is shaped like an X to reduce the size of the component. This link is 4.8 cm long and 5.7 cm broad with a thickness of 8 mm.

Base link: This part connects the middle link to the body of the robot. This part also connects the top of the robot to the bottom. It holds one motor which is used to drive the middle link. The motor will be screwed into the slot made for it. It is 6.3 cm long and 4.15 cm broad with a thickness of 8mm.

Connector: The connector is used to connect the links and the back of the motor. The connector is joined to the motor and the cylindrical part, which is inserted into the slots made in the links. This part ensures better stability during motion

and reduces stress at the end of the links where the rotor of the motor is fixed.

Base Plate: The base plate is used to hold the electronic components. It has six slots for the motors to be mounted which are connected to the base link. The plate has an edge length of 7.92 cm and a thickness of 4 mm. The plate is made into three parts which are joined together. The three parts are made such that they form a lap joint with each other. The parts are connected using a 3D pen. Slots of different shapes have been made on the plate to reduce the weight of the part.

Top plate: The top plate is used to cover the electronic components from the environment over it. It has the same dimensions as the base plate. It has cylindrical extrusions for joining the base link. Like the base plate, the top plate is made by joining three separate identical parts with a 3D pen. The slots in the base plate are mainly for weight reduction.

B. Structural Analysis of Proposed Spiderbot

Structural analysis evaluates how proposed design performs under real-world loading conditions. Authors have used ANSYS software to analyze each design component. The structural performance varies mainly due to the forces on the components, their material and geometry. All components used in this research are made of plastic. In this paper, the total deformation, equivalent (Von-Mises) elastic stress, and equivalent (Von-Mises) stress were analyzed. Structural stress loading [19] could be monitored for better analysis and solid performance. From the analysis, authors observed that all the components used can withstand the load conditions without failure, hence they can be the best choice for the proposed robot.

The deformations shown in Fig. 4 to Fig. 8 below are an exaggerated view. The different colour codes are used to understand the range of the characteristic throughout the part which is being analysed. Red being the maximum and dark blue being the minimum (as shown in the legend). Therefore, the deformation of the parts cannot be noticed in real life. The results we drew have three characteristics in discussion at very negligible ranges.

Top Plate: The only forces that the top plate experiences are from the rotation of the base link which is driven by the motor. The forces of rotation are applied on the cylindrical structures of the plate. The rotational velocity applied is 9.5 rad/s. There are no other forces acting on the top plate, as shown in Fig. 4.

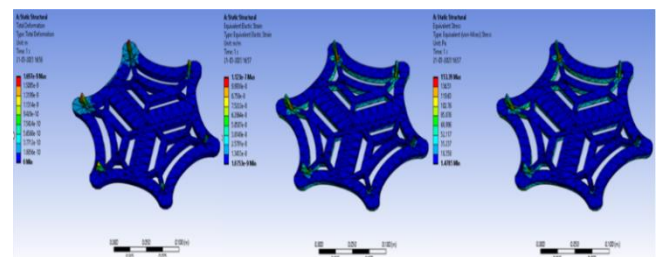


Fig. 4. Structural deformation analysis, equivalent elastic strain, and equivalent (Von-Mises) stress of the top plate 3D design

Base link: This link connects the top and bottom plates. It experiences a force of rotation at two of its slots. One slot of the link is fixed to the rotor of the motor and the other is fixed to the top plate. The rotational force experienced is 9.5 rad/s

which is generated by the motor. This rotational velocity is applied at the slots, as shown in Fig. 5.

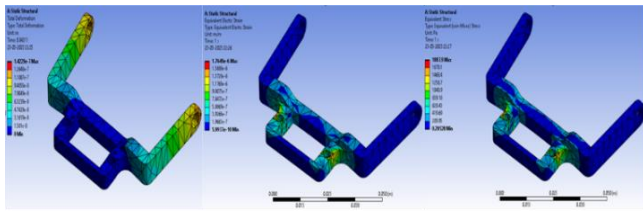


Fig. 5. Structural deformation analysis, equivalent elastic strain, and equivalent (Von-Mises) stress of the base link 3D design

X Middle Link: This link connects the base link and motors and has two motors fitted in it. It experiences rotational velocity in 4 of its slots. Two slots experience force from the motor and the other two from the connector. The motor generates a rotational velocity of 9.5 rad/s. This force is applied at the four slots in the design, as shown in Fig. 6.

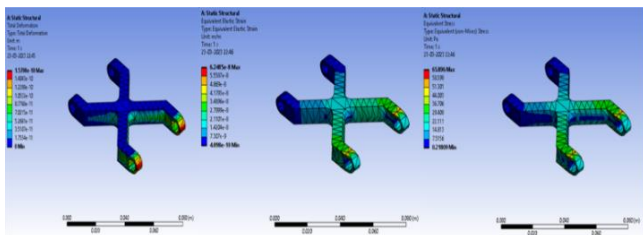


Fig. 6. Structural deformation analysis, equivalent elastic strain, and equivalent (Von-Mises) stress of the middle link 3D design

Base Plate: The weight of the components placed in the base plate is applied. The total weight of electronic components is 271.5 g. The base plate holds all the electronic components and must not fail under the forces applied on it. The weight is equally distributed among the three parts, which the base plate comprises of, as shown in Fig. 7.

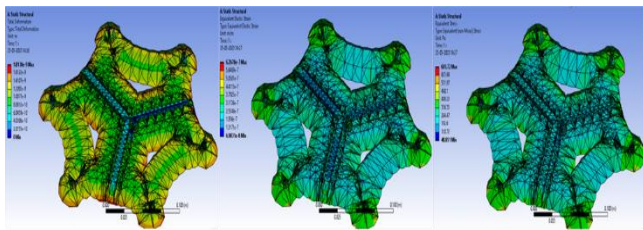


Fig. 7. Structural deformation analysis, equivalent elastic strain, and equivalent (Von-Mises) stress of the base plate 3D design

Legs: The leg is a very vital component of the design. It is essential for the legs to be able to withstand the entire weight of the robot. Also, since the tips that encounter the ground have a small area of contact, the pressure developed at the tips is high. This may cause failure of the leg. We must ensure that the legs do not fail under these conditions. The load of the

$$H3^0 = \begin{bmatrix} C1(C2C3 - S2S3) & -C1(C2S3 + S2C3) & S1 & C1[L3C2C3 - S2L3S3 + L2C2 + L1] \\ S1(C2C3 - S2S3) & -S1(C2S3 + S2C3) & -C1 & S1[L3C2C3 - L3S3S2 + L2C2 + L1] \\ S2C3 + C2S3 & -S3S2 + C2C3 & 0 & L3[C3S2 + S3C2] + L2S2 \\ 0 & 0 & 0 & 1 \end{bmatrix} \quad (1)$$

entire weight of the robot is given at the tip of the leg, as shown in Fig. 8.

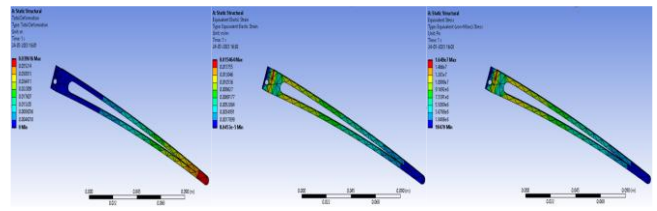


Fig. 8. Structural deformation analysis, equivalent elastic strain, and equivalent (Von-Mises) stress of the Spider legs 3D design

C. Kinematic Analysis of Spiderbot

The architecture of optimal leg alignments is vital for a spiderbot's efficient operation. The physical constraints of the spiderbot's legs determine the core aspects of its movement. Selecting a leg design that provides maximum support with an extensive range of motion is essential, as it should not impose unnecessary limitations on the robot's maneuverability [21].

1) Forward Kinematics

The Denavit-Hartenberg (DH) algorithm is applied to one of the spiderbot legs to acquire the kinematics of the robot under study. Generally, both the four or six-legged robot utilize the same leg configurations that are symmetrically arranged and have three degrees of freedom (DOF) as shown in Fig. 9. The homogeneous transformation matrices that relate a link and its joint movements in matrix form are created by DH data parameters. But for the proposed spiderbot, authors have considered 3DOF leg having 3 joints as shown in fig. 9 where, the base link joint is responsible for performing the yaw movement of link 1 and the remaining middle link and leg link joints are responsible for pitch movements. The obtained DH table by applying frames at each joint is shown in Table I. The homogeneous transformation matrix obtained from the DH table provides the position of the edge or leg tip in x, y, and z directions are listed as px, py, and pz below in Eq. (1).

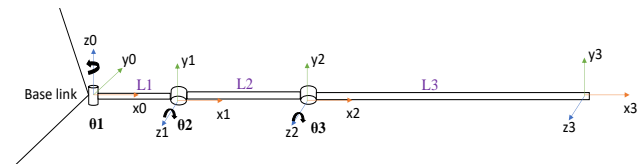


Fig. 9. Kinematic diagram of Single-Leg

TABLE I. DH-PARAMETERS

n	d(z-1)	θ(z-1)	αx	rx
1	0	θ1	90°	L1
2	0	θ2	0	L2
3	0	θ3	0	L3

$$\begin{aligned}
 P_x &= C_1 [L_3 C_2 C_3 - S_2 L_3 S_3 + L_2 C_2 + L_1] \\
 P_y &= S_1 [L_3 C_2 C_3 - S_2 L_3 S_3 + L_2 C_2 + L_1] \\
 P_z &= L_3 [C_3 S_2 + S_3 C_2] + L_2 S_2
 \end{aligned}$$

By using the DH parametrized homogeneous transformation matrix, authors tried to program the equations by including the link lengths and rotation angles for each joint. Hence, each link tip position with respect to its joint is obtained as shown in Fig. 10. The first joint can give better position within 0-100 degree because of the movement constraints. Whereas the middle link can give better movement between 0-60 degree and similarly the leg portion can give better movement between 0-80 degree.

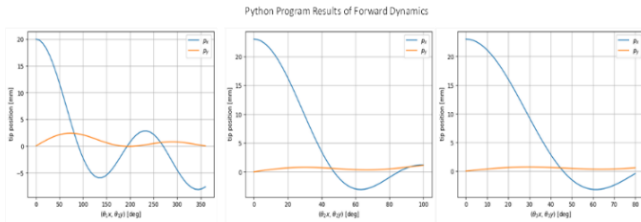


Fig. 10. Tip position in X And Y directions with respect to each joint

2) Inverse Kinematics

The graphical approach of inverse kinematics calculations is considered for Fig. 11 to obtain its angle of movements at each joint. The corresponding calculations are obtained for both top view approach (as obtained in equations (2), (3) and (4)) and side view approach.

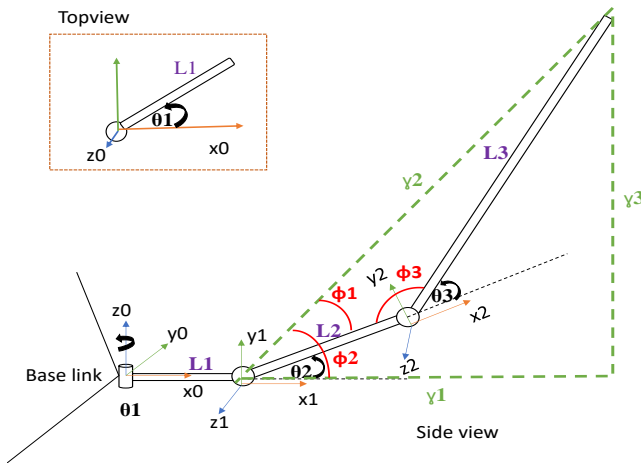


Fig. 11. Top and side view of the spiderbot leg consideration for inverse kinematics

Top View:

$$\theta_1 = \tan^{-1}(Y/X) \tag{2}$$

Side View (3):

$$J = \begin{bmatrix} R_0^0 \begin{bmatrix} 0 \\ 0 \\ 1 \end{bmatrix} X(d_3^0 - d_0^0) & R_0^0 \begin{bmatrix} 0 \\ 0 \\ 1 \end{bmatrix} X(d_3^0 - d_1^0) & R_2^0 \begin{bmatrix} 0 \\ 0 \\ 1 \end{bmatrix} X(d_3^0 - d_2^0) \\ R_0^0 \begin{bmatrix} 0 \\ 0 \\ 1 \end{bmatrix} & R_0^0 \begin{bmatrix} 0 \\ 0 \\ 1 \end{bmatrix} & R_2^0 \begin{bmatrix} 0 \\ 0 \\ 1 \end{bmatrix} \end{bmatrix} \begin{bmatrix} \theta_1 \\ \theta_2 \\ \theta_3 \end{bmatrix} \tag{5}$$

$$\begin{aligned}
 \phi_2 &= \tan^{-1}(y_2 / y_1) \\
 \theta_2 &= \phi_2 - \phi_1 \\
 \theta_2 &= [\tan^{-1}(y_2 / y_1)] - \cos^{-1} \{ [(L_3)^2 - (L_2)^2 - (y_3)^2] / [2(L_2)(y_3)] \} \tag{3}
 \end{aligned}$$

$$\begin{aligned}
 \theta_3 &= 180^\circ - \phi_3 \\
 y_3^2 &= (L_2)^2 + (L_3)^2 - 2L_2L_3 \cos \phi_3 \\
 \phi_3 &= \cos^{-1} [(L_2)^2 + (L_3)^2 - (y_3)^2] / (2L_2L_3) \\
 \theta_3 &= 180^\circ - \cos^{-1} (y_3^2 - L_2^2 - L_3^2 / 2L_2L_3) \tag{4}
 \end{aligned}$$

3) Jacobian Velocity Propagation Analysis

The Velocity Propagation Method (VPM) is a strategy that is considered and developed for determining the linear and angular velocities of joint link motions. The velocity propagation method is employed on the kinetic structure as in Fig. 9 and Fig. 11. The estimated Jacobian matrix for the spiderbot leg was designed before, by applying the rules governing the VPM table in detail as in from eq. (5) and (6).

From the obtained Jacobian velocity propagation matrix, it is proved that the rotation of spiderbot leg tip in z0 axis rotation is controlled by (theta1) moment, Y0 axis rotation by theta2 + theta3 by L2 and L3 respectively and X0 axis rotation by nothing (means there is no movements).

III. MODELLING AND SIMULATION OF LEG JOINTS IN SIMSCAPE MULTIBODY

Obtaining an expression for the individual dynamics of a single limb of the hexapod robot is relatively simple, but the hexapod robot has six legs, for a total of 18 DOF. Consequently, a single leg's dynamics are adequate to calculate, as it is understood that the same will be applied to the remaining legs. As a result, authors utilized the MATLAB tool Simscape Multibody, which has the advantage of performing simulations using blocks that depict links and joints (rotational or prismatic), as though the robot were being assembled. A single leg is designed in Simscape Multibody as shown in Fig. 12 and simulations were performed on it. Signal builders are employed to generate three step signals, which are then provided to the spider leg design as joint angles for its movement as in Fig. 13 and Fig. 14. First signal within the signal constructor is a 0.2-amplitude step signal that activates at 4 seconds, causing the first joint to move with a step of 0.2 radians at 4 seconds. Similarly, the second and third step signals of 1 radians amplitude activate the second and third joint at 5 seconds. At the PD controller, these step signals are deemed reference signals as depicted in Fig. 15. These joint stages are used to generate torque at each leg joint to generate movement. With the intention of attaining a feed forward compensator, a 2 DOF PD controller with reference configuration and tuning has been implemented.

$$= \begin{bmatrix} S_1(L_3C_2C_3 - L_3S_3S_2 + L_2C_2 + L_1) & L_3(C_3S_2 + S_3C_2) + L_2S_2 & L_3(C_3S_2 + S_3C_2) \\ C_1(L_3C_2C_3 - S_2L_3S_3 + L_2C_2 + L_1) & 0 & 0 \\ 0 & [-C_1(L_3C_2C_3 - S_2L_3S_3 + L_2C_2)] & C_1(L_3C_2C_3 - S_2L_3S_3) \\ \begin{bmatrix} 0 \\ 0 \\ 1 \end{bmatrix} & \begin{bmatrix} 0 \\ 1 \\ 0 \end{bmatrix} & \begin{bmatrix} 0 \\ 1 \\ 0 \end{bmatrix} \end{bmatrix} \begin{bmatrix} \theta_1 \\ \theta_2 \\ \theta_3 \end{bmatrix}$$

$$J = \begin{bmatrix} \dot{x} \\ \dot{y} \\ \dot{z} \\ w_x \\ w_y \\ w_z \end{bmatrix} = \begin{bmatrix} [-S_1(L_3C_2C_3 - L_3S_3S_2 + L_2C_2 + L_1)]\dot{\theta}_1 + [L_3(C_3S_2 + S_3C_2) + L_2S_2]\dot{\theta}_2 + [L_3(C_3S_2 + S_3C_2)]\dot{\theta}_3 \\ [C_1(L_3C_2C_3 - S_2L_3S_3 + L_2C_2 + L_1)]\dot{\theta}_1 \\ [-C_1(L_3C_2C_3 - S_2L_3S_3 + L_2C_2)]\dot{\theta}_2 + C_1(L_3C_2C_3 - S_2L_3S_3)\dot{\theta}_3 \\ 0 \\ \dot{\theta}_2 + \dot{\theta}_3 \\ \dot{\theta}_1 \end{bmatrix} \quad (6)$$

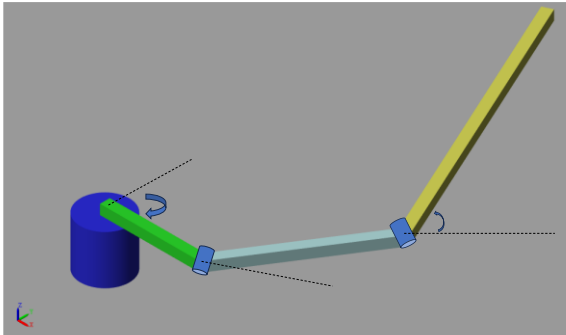


Fig. 12. Isometric view of individual leg modelling in SIMSCAPE

To test the PID controller, the PD blocks in the preceding SIMSCAPE model are replaced with PID blocks, and the obtained results for the same set of step inputs are depicted in Fig. 17. However, only at joint 1, can minor variations be observed; consequently, the PID controller has been auto-tuned to achieve the desired results. After fine-tuning PID, the desired output has been flawlessly realized as shown in Fig. 18.

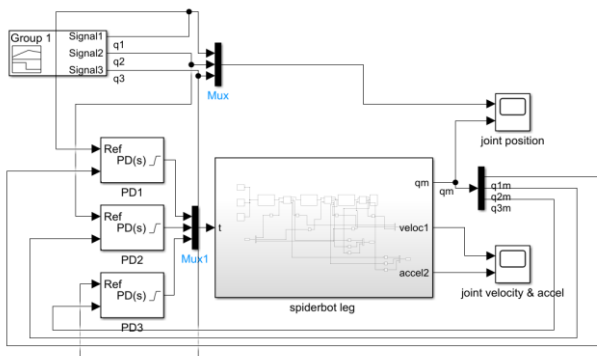


Fig. 13. PD controller modelling for spiderbot leg in SIMSCAPE multibody

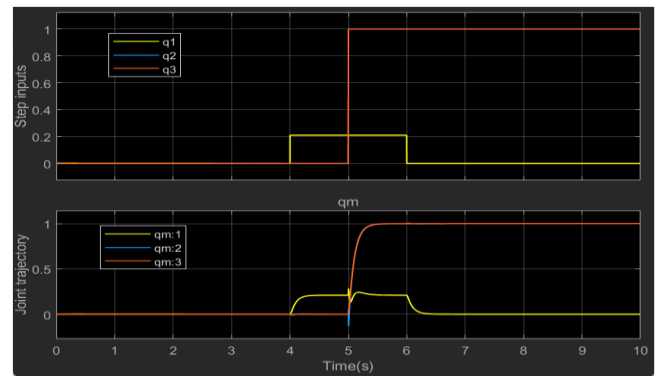


Fig. 15. Single leg 3 joints position trajectory response obtained with respect to given step inputs for PD controller (without tuning at P = 124.12, and D = 12.594)

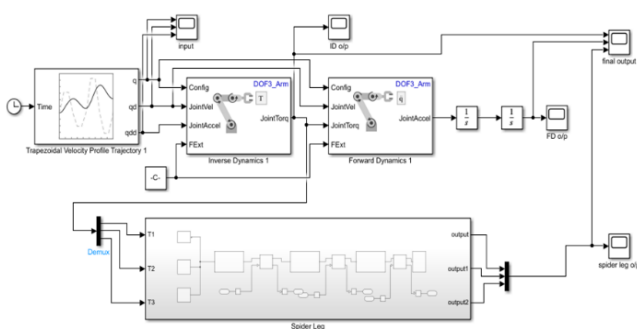


Fig. 14. Trapezoidal velocity profile trajectory analysis, for forward and inverse dynamics for spiderbot leg trajectory planning

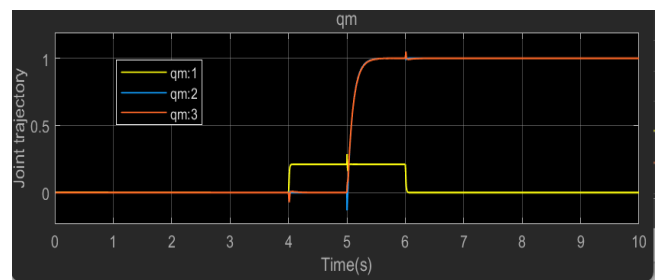


Fig. 16. Single leg 3 joints position trajectory response of step inputs for PD controller (after tuning P=8888.64, and D = 75.47)

The joint position trajectory obtained by the PD controller, as depicted in Fig. 15, has minor deviations at joints 1 and 2 relative to the reference signal. Therefore, only PD1 underwent automatic tuning, and the results obtained were in line with expectations. Changes at P and D values are highlighted in Fig. 16, labelling after refining.

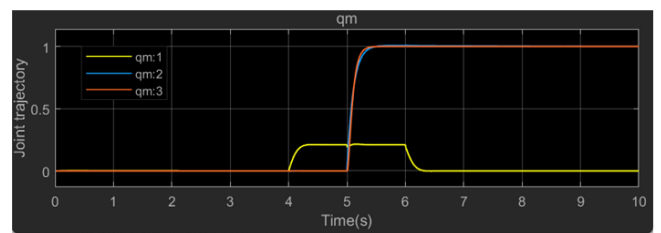


Fig. 17. Single leg 3 joints position trajectory response of step inputs for PID controller (without tuning P=4561.82, I= 32038.46, and D = 221.58)

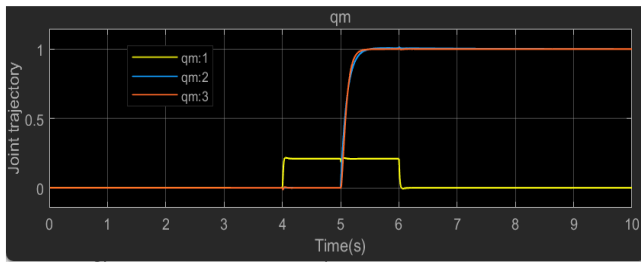


Fig. 18. Single leg 3 joints position trajectory response of step inputs for PID controller (after tuning $P=4833.588$, $I=101212.7$, and $D=49.712$)

Contrasting the tuned PD controller with the PID controller (from Fig. 15 to Fig. 18), authors can conclude that the exact output that is necessary is achieved with the PID controller. Whereas, in PD controllers, even after tuning at PD1, there are still some variances at joint 2, which may necessitate tuning at PD2 as well. In contrast, the proposed design considers the four legs to be 3 DOF joint link connections, while the remaining two legs are 2 joint connections. This proposed (4 + 2) six-legged spiderbot's movement angles are contrasted with all its legs with respect to time in a later section of this paper.

The Trapezoidal velocity profile of the trajectory analysis, for forward and inverse dynamics of spiderbot leg trajectory planning has been performed in SIMSCAPE, as in Fig. 14. The input displacement, velocity, and acceleration with respect to acceleration phase, cruise phase and deceleration phase of segments are represented in Fig. 19. The displacement amplitudes are considered between 0-0.35 range. Whereas the velocity is negative at segment I and III, but positive at segment II.

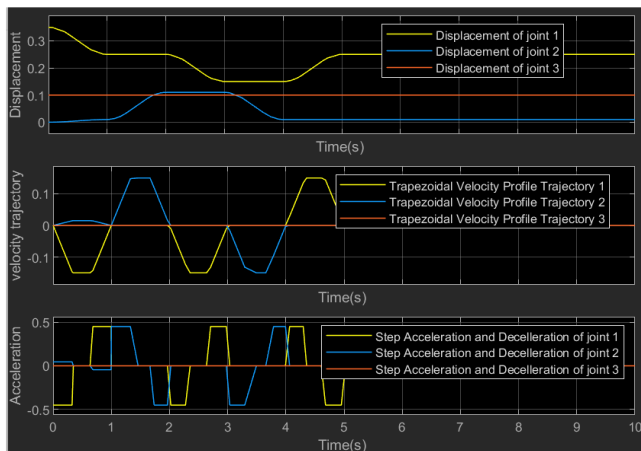


Fig. 19. Trapezoidal velocity profile trajectory having displacement, velocity and acceleration profiles have been provided for the spiderbot leg as an input

The step signal represents decelerating at segment I, zero at segment II and accelerating at segment III. The output obtained with respect to all the three joints can be observed at Fig. 20. Where the torque obtained at Inverse dynamics is influenced by all the displacement, velocity and acceleration can be seen in Fig. 20. The forward dynamics influenced by the inverse dynamics provides the trajectory of all the three joints in the required movement, when compared to simple spiderbot leg simulation trajectory.

The simulation results, depicted in Fig. 15 through Fig. 17, highlight the effectiveness of the PID controller in addressing the minor deviations observed with the PD controller. The

fine-tuning process for the PID controller demonstrates its ability to minimize these deviations, resulting in smoother trajectory adherence. While deviations at joints 1 and 2 under the PD controller were minor, they could potentially impact the robot's ability to maintain precise trajectories during complex maneuvers or in uneven terrains.

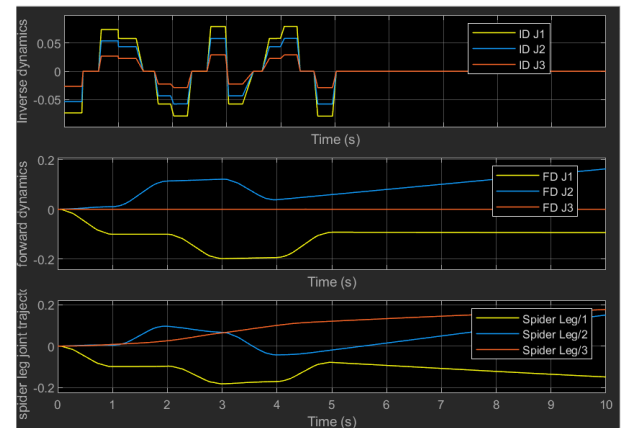


Fig. 20. Output obtained from the spiderbot leg simulations for inverse dynamics, forward dynamics, and spider leg trajectory

IV. HARDWARE IMPLEMENTATION OF PROPOSED SPIDERBOT

The spiderbot with the use of MG90s motors which is light weighted and provides more torque, PCA9685 as shield for multiple servo driver and Raspberry Pi Pico as the controller having 26 GPIO pins where 16 are PWM controllers, 2 UARTs, 2 I2C and 8 programmable input/output state machine custom peripheral support powered by Li-Ion batteries [22], [45]. In Hexapod robot use of motor – Hitech HS-645Mg servo motor as it offers the strongest gear train comparatively, powered and controlled by Arduino Mega 2560 54 digital input/output of which 15 can be PWM outputs, 16 as analog inputs and 4 UARTs [28]. Journal of Hexapod Robot with Maneuverable Wheel, the six legs are controlled by PIC (Programmable Integrated Circuit) running through MikroC Program Code and 14 servo motors (C36R and C40R) connected to SC16A – 16 channel servo controllers [46]-[50]. Hexapod article has implemented image acquisition bot using Arduino uno controller having 14 digital input/output of which are PWM outputs with operating voltage of 5V controlling SG90s motors weighing 9g each and stall torque of 1.8 kgf/cm [29]-[30].

RHex Hexapod [5], is a different robot compared to other hexapod robots as it uses DC motors for actuating. The motors that are used at this robot are Maxon type motors with a 33:1 planetary gearhead powered by a 24V NiMH battery and controlled by RHio PC10 in software environment RhexLib [5]. The hexapod used smart actuator module Dynamixel RX-28 joint actuators producing high torque despite its small size which are controlled by ATmega128 communicated with RS232. The hexapod robot, Bill-Ant-P robot manufactured using 6061 aluminum and carbon fiber sheets, uses MPI MX-450HP hobby motors for its reliability, high torque, and affordability movement as they have 8.37kg-cm of torque, can rotate about 60 degrees in 0.18sec, and has a small internal DC motor consumes 1125mW of power at stall torque connected to IsoPod microcontroller. There are eight ADC inputs on the IsoPod™, six of which are used to measure foot-mounted sensor forces and two Acroname BrainStem GP 1.0

microcontrollers are used in the head which have four R/C servo output, five 10-bit ADC inputs, five digital I/O ports, an RS-232 serial interface, I2C interface bus, and a digital IR range finder input which are powered by four on-board 2400mAh, 7.4vdc Li-ion batteries and to limit the voltage to 6.0vdc, each of the batteries is connected to an MPI ACC134 6-volt Regulator.

Motor: There are plenty of motors available in the aspect of movement such as AC motors, DC motors, Stepper motor, Servo motor, and more. The authors selected MG90s servos due to their lightweight, high torque, and cost-effectiveness, as depicted in Fig. 21, which is a micro servo motor with metal gear with high output power and rotation of about 180°. MG90s is picked over other motors as it has a PWM frequency of 50Hz, has better torque than SG90, is lightweight, and is inexpensive. The authors aim to use 14 servo motors for the locomotion of the robot, where each servo motor represents the leg joint of the robot. Both the front and back legs having 3 joints each and middle legs having 2 joint each sums up to 14 servo motors. The robot balances on 3 feet at once during the motion. The MG90s motor works for input voltage of 4.8v to 6v, stall torque 1.8 kg/cm, rotation 0°-180°, speed 0.12s/60°, weight of motor 13.4grams.

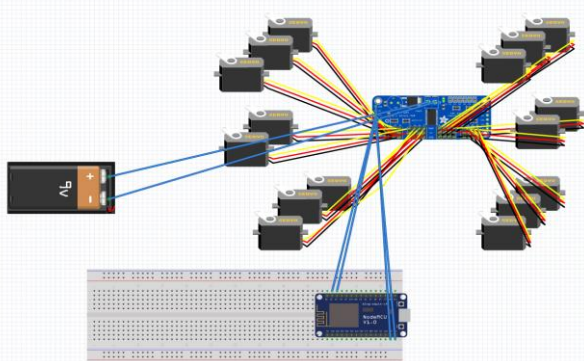


Fig. 21. Electric circuit connections of the servomotors with mode MCU

PCA96850: The role of controller is to direct the servo motors. The controller used here is PCA9685, 16-channel servo driver which can control up to 16 individual servo motors and uses I2C communication protocol which can connect and control multiple slaves from a single master. 6 address select pins so one can wire up to 62 of these on a single I2C bus, a total of 992 outputs. It has operating voltage between 3.3v to 5v (3.3v logic pull up). Adjustable frequency PWM up to about 1.6 KHz.

ESP8266: It has 17 GPIO pins and communicates with PCA9685 using I2C communication protocol. The SCL (I2C clock pin), SDA (I2C data pin) pins of PCA9685 is connected to the D1, D2 pin of the board respectively, and VCC is the logic pin which should have voltage between 3-5V. Authors preferred this board as it's also capable to act a Wi-Fi module where it can establish the wireless connection and give instruction using the device connected to the same Wi-Fi connection.

Power required: Multiple servo motors will be high considering that providing a high amount of voltage shouldn't damage the controller board or the servo. Hence, authors use a 9v alkaline battery as in Fig. 21 which is rechargeable and inexpensive for multiple use which gives ideal voltage to all the servo's connected. In case of using other power supply

with lesser or higher voltage, one can implement voltage regulator to bring up or down the voltage as required.

The program for the movements of the robot is loaded to the ESP8266 board using Arduino IDE software. Initially all the servo motor is set to 90° as the reference angle. The movements which are implemented in this robot is to move forward, backward, left, right and depending on the direction, the angles of the servo motor change respectively. The method of walking forward is called GAIT and the type of gait implemented here is called Tripod Gait (it is chosen for its superior stability, moderate speed, and energy efficiency, making it ideal for tasks that require both agility and reliable performance), where the hexapod always has 3 feet in contact with the ground, which are the front and back legs of one side and middle leg of the other side. The middle servo determines whether the leg will be lifted or placed on the earth. For instance, for moving forward, the robot moves front by pushing those feet against the earth backwards while the other set of legs are moving forward in air. The robot walks forward by constantly distributing its weight between the middle legs and elevating the feet [51]-[52].

From military applications to industry and household activities, robotics plays a significant role. Among the most implemented robots for locomotion tasks across various terrains are four-legged (quadrupedal) and six-legged (hexapod) robots. These robots are often preferred over wheeled robots because they are not limited to smooth surfaces, can avoid or jump over obstacles, and traverse difficult terrain more easily. The design and proposed use of these robots depend on their intended purpose and functionality. In this article, authors compare four-legged and six-legged robots based on various factors that highlight their performance and capabilities.

By making use of the physical circuit connections like in Fig. 22, for four leg actuations with 12 motor and six leg actuations with 16 motors (where four legs with 3 motors each, remaining two legs with 2 motors each), authors able to obtain the variation in joint angles of 3 motors of each leg are as shown in Fig. 22 and Fig. 23. The authors tried to validate the angle of movement and individual joint movements of legs variations depending on the number of legs, which are used for its movements with respect to time.

By making use of 3D printer, the Spiderbot as shown in Fig. 25 is fabricated. Also, performed few modifications in its leg design with 3D pen for providing grip/ strength to hold over all robot on its four legs. The load carrying capacity of the proposed 6 leg bot with 3 joints at four legs and 2 joints at two legs as in Fig. 25 is 3.5 kg as max (including battery, controller etc). The structural movement of Spiderbot is awaiting a comprehensive vibration analysis [53] to be conducted (will assess factors like vibration frequencies, amplitude, resonance, and damping efficiency. By addressing issues such as mechanical imbalances and resonance, performance, stability, and energy efficiency can be improved. This leads to enhanced precision, longer lifespan, and smoother operation). This analysis will provide insights into the dynamic behaviour of the structure with environmental impacts [54] on it, ensuring its stability and performance.

From the Fig. 24, the calculated Root Mean Square Error (RMSE) reflects how well the actual trajectory matches the reference. For stability analysis the RMSE is 0.0463. For

energy efficiency analysis, the estimated energy consumption is 2.6508 units. For task-specific performance, the system is highly stable with minimal deviations. The results from Fig. 24 suggest that achieving a low RMSE is critical for ensuring the robot's stable operation, especially in tasks requiring precision, such as obstacle avoidance or path-following. The energy metric provides insights into the robot's efficiency, aiding in optimizing power consumption for extended operational periods. Together, these metrics enable researchers to balance stability, efficiency, and task-specific needs, ensuring robust and reliable robotic performance.

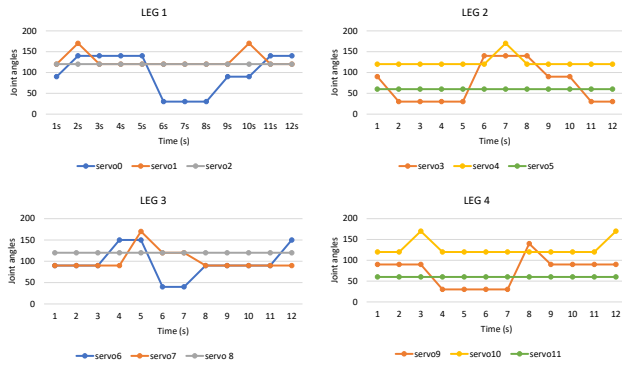


Fig. 22. Four leg bot joint angle position analysis with respect to time

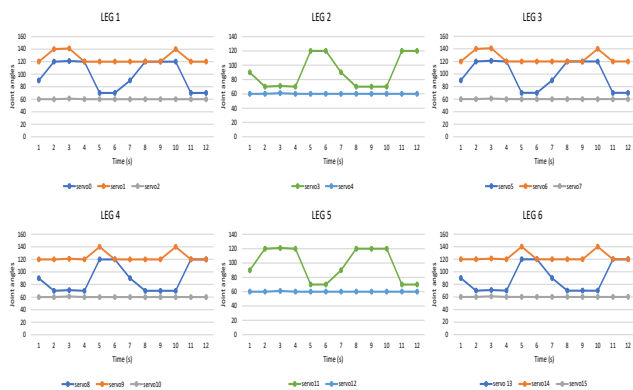


Fig. 23. Six-legged bot joint angle position analysis with respect to time

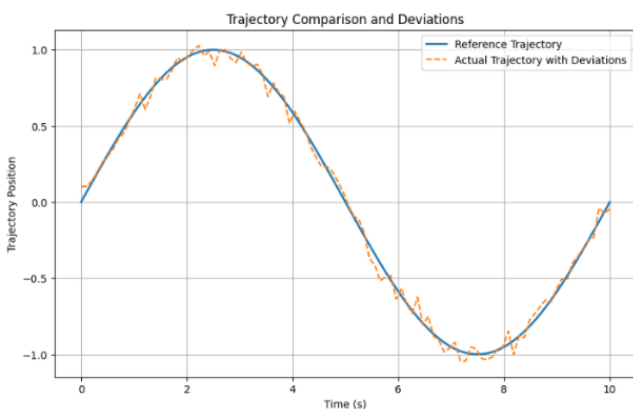


Fig. 24. Trajectory Comparison: Reference vs. Actual with Deviations

Four-Legged Bot: According to [1], quadrupedal robots, like the one in [21], mimic the locomotion patterns of common animals such as dogs and lions. They can also adopt specialized gaits, such as the creep gait, for specific needs. These robots are noted for their stability both when stationary and in motion. In [2], quadrupedal robots are categorized

based on their actuation methods, and their performance is compared across different performance factors.

Six-Legged Bot: The paper [1] presents the concept of hexapods, which are inspired by insects and their multiple gaits. Hexapods can maintain stability even with three legs in the air while the other three support the body's weight on the ground, as discussed in [22] and [51].



Fig. 25. 3D Printed Spiderbot Design (4 Leg Actuated)

As in the name, four-legged bot is simple to design and manufacture mimicking the animal as a pair in front and back. Whereas the six-legged bot would put you in a place of complex designing the placement of legs like either three legs in each side or two legs in each side and one in the front and remaining one at the back. In paper [55], which discusses about the stability of various bots classifies stability in two types as: Static stability and Dynamic stability. Both having 3 DOF, four-legged bot [56] lacks stability while being static or slow locomotion where it requires at least 3 legs placed at the surface and six-legged bot takes advantage of this feature and remains statically stable having greater center of gravity. While in motion, four-legged bot has greater dynamic stability compared to six-legged bot as its movements are quicker than six-legged bot.

Despite having lesser legs/support, four-legged bot has higher payload capacity (2.8 kg maximum) as it has bigger or wider base as lesser center of gravity which allows to carry more load during locomotion. six-legged bot moves faster and efficiently than the four-legged alongside lacking stability, where if the application requires speed over stability, then, six-legged bot (payload capacity 3.5 kg maximum) will be preferred. Having extra pairs of leg, it makes six-legged bot to navigate and traverse easier than the four-legged bot making it move more than the definite direction. Focusing only on the locomotion the bot, each having three DOF, six-legged bot drains more power than four-legged as it implies more servo motors as per use. In case of damage or failure of one leg or joint, the six-legged bot can sustain in that specific case than 4-legged bot to further move on with the locomotion and application. Selection of bot for application depends on diverse factors which we imply based on necessities, where if we focus on stability application during motion then 4-legged bot gives better and efficient performance comparatively, used in recovery mission and military purposes. When the application focuses on maneuverability and speed, six-legged bot comes in action for purpose of surveillance, inspection, and investigation missions [57]–[61].

This study aims to address the challenges of existing spider robots, such as high complexity, cost, and inefficiency, by introducing a simplified and modular design. By reducing the number of motors and links, the proposed robot achieves a balance between performance and practicality, enabling applications in hazardous environments where stability, agility, and cost-effectiveness are paramount. Unlike conventional designs with up to 24 degrees of freedom, this research explores configurations with four and six legs, ensuring adaptability for diverse terrains while leaving room for integrating advanced functionalities like pick-and-place robotic arms. This study distinguishes itself through the application of kinematic analysis, PID-controlled movement optimization, and real-time simulation using SIMSCAPE Multibody. The modular approach not only streamline fabrication but also paves the way for customizable robots suited for specific tasks such as obstacle avoidance or material handling. By presenting a well-structured design framework and empirical validation, this research contributes significantly to the field of bio-inspired robotics, pushing the boundaries of legged robotic applications in hazardous and inaccessible areas.

V. CONCLUSION

Both four- and six-legged robots have their own advantages and disadvantages depending on the chosen application. Therefore, the efficiency of the robot is determined by its application. This study aims to simplify the design and circuitry to create a more concise and efficient robot. We considered the forward and reverse kinematics of a single limb, including joint velocity derivations, for the proposed connections. A 3D CAD model was created in Fusion 360 and analyzed for deformation, tension, and strain. The parts were manufactured using a 3D printer with FDM process and PLA material. SIMSCAPE Multibody in MATLAB was used to study the single leg 3DOF design with PD and PID control. Simulations were conducted to investigate configurations with four and six legs, using a model connected to a servomotor and controlled in SIMSCAPE. The evaluation focused on the robot's speed and stability with the reduced limb design. Future work will involve replacing two legs with robotic arm structures for pick-and-place operations and obstacle avoidance, enabling further bio-inspired advancements. Future work will also focus on conducting rigorous performance tests to derive quantitative metrics, such as movement speed and stability under varying loads etc. These innovative approaches contribute to the advancement of bio-inspired robotics, providing a robust solution for detecting and responding to hazardous situations in inaccessible areas.

ACKNOWLEDGMENT

This work is supported by the University Putra Malaysia and Manipal Institute of Technology.

CONFLICTS OF INTEREST

The authors declare that the research was conducted in the absence of any commercial or financial relationships that could be constructed as a potential conflict of interest.

REFERENCES

- [1] C. Sun, M. Yuan, F. Li, Z. Yang, and X. Ding, "Design and simulation analysis of hexapod bionic spider robot," in *Journal of Physics: Conference Series*, vol. 1168, no. 2, p. 022094, 2019.
- [2] R. D. Shi, X. L. Zhang, and Y. A. Yao, "A CPG-based control method for the multi-mode locomotion of a desert spider robot," *Robot*, vol. 40, no. 2, pp. 146-157, 2018.
- [3] Y. Zhang, Y. Qian, Y. Ding, B. Hou, and R. Wang, "Adaptive walking control for quadruped robot by using oscillation patterns," *Scientific Reports*, vol. 13, no. 1, p. 19756, 2023.
- [4] V. V. Kravchenko *et al.*, "Comparison of Spider-Robot Information Models," *Journal of Robotics and Control (JRC)*, vol. 4, no. 5, pp. 719-725, 2023.
- [5] Y. Zhang, G. Qiao, Q. Wan, L. Tian, and D. Liu, "A novel double-layered central pattern generator-based motion controller for the hexapod robot," *Mathematics*, vol. 11, no. 3, p. 617, 2023.
- [6] A. H. Abdulwahab, A. Z. A. Mazlan, A. F. Hawary, and N. H. Hadi, "Quadruped robots mechanism, structural design, energy, gait, stability, and actuators: a review study," *International Journal of Mechanical Engineering and Robotics Research*, vol. 12, no. 6, 2023.
- [7] Z. Tang, P. Qi, and J. Dai, "Mechanism design of a biomimetic quadruped robot," *Industrial Robot: An International Journal*, vol. 44, no. 4, pp. 512-520, 2017.
- [8] R. Vidoni and A. Gasparetto, "Efficient force distribution and leg posture for a bio-inspired spider robot," *Robotics and Autonomous Systems*, vol. 59, no. 2, pp. 142-150, 2011.
- [9] E. Z. Moore. *Leg Design and Stair Climbing Control for the RHex Robotic Hexapod*. Department of Mechanical Engineering McGill University, 2002.
- [10] B. Gassmann, K. -U. Scholl, and K. Berns, "Locomotion of LAURON III in rough terrain," *2001 IEEE/ASME International Conference on Advanced Intelligent Mechatronics. Proceedings (Cat. No.01TH8556)*, vol. 2, pp. 959-964, 2001, doi: 10.1109/AIM.2001.936810.
- [11] E. Burkus and P. Odry, "Autonomous Hexapod Walker Robot "Szabad(ka)"", *2007 5th International Symposium on Intelligent Systems and Informatics*, pp. 103-106, 2007, doi: 10.1109/SISY.2007.4342633.
- [12] R. Shi, X. Zhang, Y. Tian, S. Dong, and Y. Yao, "A CPG-based control method for the rolling locomotion of a desert spider," *2016 IEEE Workshop on Advanced Robotics and its Social Impacts (ARSO)*, pp. 243-248, 2016, doi: 10.1109/ARSO.2016.7736289.
- [13] F. Asadi, M. Khorram, and S. A. A. Moosavian, "CPG-based gait transition of a quadruped robot," *2015 3rd RSI International Conference on Robotics and Mechatronics (ICROM)*, pp. 210-215, 2015, doi: 10.1109/ICRoM.2015.7367786.
- [14] H. Yu, H. Gao, L. Ding, M. Li, Z. Deng, and G. Liu, "Gait Generation With Smooth Transition Using CPG-Based Locomotion Control for Hexapod Walking Robot," in *IEEE Transactions on Industrial Electronics*, vol. 63, no. 9, pp. 5488-5500, Sept. 2016, doi: 10.1109/TIE.2016.2569489.
- [15] Y. Zhang and T. Yasuno, "Adaptive walking control for quadruped robot on irregular terrain based on CPG network," *Journal of signal processing*, vol. 15, no. 4, pp. 315-318, 2011.
- [16] Y. She, C. Li, J. Cleary, and H.-J. Su, "Design and fabrication of a soft robotic hand with embedded actuators and sensors," *Journal of Mechanisms and Robotics*, vol. 7, no. 2, p. 021007, 2015.
- [17] M. Z. A. Rashid, M. S. M. Aras, A. A. Radzak, A. M. Kassim, and A. Jamali, "Development of hexapod robot with manoeuvrable wheel," *International Journal of Advanced Science and Technology*, vol. 49, 2012.
- [18] P. Biswal and P. K. Mohanty, "Development of quadruped walking robots: A review," *Ain Shams Engineering Journal*, vol. 12, no. 2, pp. 2017-2031, 2021.
- [19] K. Hauser, T. Bretl, J.-C. Latombe, K. Harada, and B. Wilcox, "Motion planning for legged robots on varied terrain," *The International Journal of Robotics Research*, vol. 27, no. 11-12, pp. 1325-1349, 2008.
- [20] I. M. Salleh, M. N. Muhtazaruddin, S. Sarip, M. Z. Hassan, and M. Y. M. Daud, "Structural health monitoring (SHM) on high stress loading of wing bracket," *Journal of Advanced Research in Applied Mechanics*, vol. 27, no. 1, pp. 16-22, 2016.
- [21] C. Urrea, L. Valenzuela, and J. Kern, "Design, Simulation, and Control of a Hexapod Robot in Simscape Multibody," *Applications from Engineering with MATLAB Concepts*, pp. 126-137, 2016.

- [22] K. Nithish, S. Amanullah, K. Akash, and H. Prasaath SP, "Spider Bot-A Quadruped Robot for Data Gathering," *Journal of Engineering Science & Technology Review*, vol. 15, no. 6, 2022.
- [23] Q. Shi *et al.*, "Development of a Small-Sized Quadruped Robotic Rat Capable of Multimodal Motions," in *IEEE Transactions on Robotics*, vol. 38, no. 5, pp. 3027-3043, Oct. 2022, doi: 10.1109/TRO.2022.3159188.
- [24] L. Wang *et al.*, "Design and implementation of symmetric legged robot for highly dynamic jumping and impact mitigation," *Sensors*, vol. 21, no. 20, p. 6885, 2021.
- [25] B. Katz, J. D. Carlo and S. Kim, "Mini Cheetah: A Platform for Pushing the Limits of Dynamic Quadruped Control," *2019 International Conference on Robotics and Automation (ICRA)*, pp. 6295-6301, 2019, doi: 10.1109/ICRA.2019.8793865.
- [26] G. Zhang, S. Ma, J. Liu, X. Zeng, L. Kong, and Y. Li, "Q-Whex: A simple and highly mobile quasi-wheeled hexapod robot," *Journal of field robotics*, vol. 40, no. 6, pp. 1444-1459, 2023.
- [27] M. Travers, A. Ansari, and H. Choset, "A dynamical systems approach to obstacle navigation for a series-elastic hexapod robot," *2016 IEEE 55th Conference on Decision and Control (CDC)*, pp. 5152-5157, 2016, doi: 10.1109/CDC.2016.7799057.
- [28] K. U. Ariawan, G. S. Santyadiputra, and I. W. Sutaya, "Design of Hexapod Robot Movement Based on Arduino Mega 2560," in *Journal of Physics: Conference Series*, vol. 1165, no. 1, p. 012011, 2019.
- [29] S. Rathnaprabha, S. Nivetha, S. Pradeepa, and S. Sindhu, "Designing of Hexapod Robot," *International Journal of Advanced Research in Electrical, Electronics and Instrumentation Engineering*, vol. 5, no. 2, 2016.
- [30] M. Nitulescu, M. Ivanescu, V. D. Hai Nguyen, and S. Manoiu-Olaru, "Designing the legs of a hexapod robot," *2016 20th International Conference on System Theory, Control and Computing (ICSTCC)*, pp. 119-124, 2016, doi: 10.1109/ICSTCC.2016.7790651.
- [31] M. M. Billah, M. Ahmed, and S. Farhana, "Walking hexapod robot in disaster recovery: developing algorithm for terrain negotiation and navigation," in *Proceedings of world academy of science, engineering and technology*, vol. 42, pp. 328-333, 2008.
- [32] M. Kurisu, "A study on teleoperation system for a hexapod robot — Development of a prototype platform," *2011 IEEE International Conference on Mechatronics and Automation*, pp. 135-141, 2011, doi: 10.1109/ICMA.2011.5985645.
- [33] A. K. Mishra. *Design, simulation, fabrication and planning of bio-inspired quadruped robot*. Requirement of the degree of Master of Technology, Indian Institute of Technology Patna: Bihar, India, 2014.
- [34] D. Huang, W. Fan, Y. Liu, and T. Liu, "Design of a Humanoid Bipedal Robot Based on Kinematics and Dynamics Analysis of Human Lower Limbs," *2020 IEEE/ASME International Conference on Advanced Intelligent Mechatronics (AIM)*, pp. 759-764, 2020, doi: 10.1109/AIM43001.2020.9158973.
- [35] L. Wang *et al.*, "Design and dynamic locomotion control of quadruped robot with perception-less terrain adaptation," *Cyborg and Bionic Systems*, 2022.
- [36] R. Barrio, Á. Lozano, M. A. Martínez, M. Rodríguez, and S. Serrano, "Routes to tripod gait movement in hexapods," *Neurocomputing*, vol. 461, pp. 679-695, 2021.
- [37] S. A. M. Esa and N. A. C. Sidik, "Design and Analysis of Vortex Induced Vibration Suppression Device," *Journal of Advanced Research Design*, vol. 85, no. 1, pp. 1-10, 2021.
- [38] N. F. C. Halim and N. A. C. Sidik, "Nanorefrigerants: A Review on Thermophysical Properties and Their Heat Transfer Performance," *Journal of Advanced Research in Applied Sciences and Engineering Technology*, vol. 20, no. 1, pp. 42-50, 2020.
- [39] C. Chun, T. Biswas, and V. Bhandawat, "Drosophila uses a tripod gait across all walking speeds, and the geometry of the tripod is important for speed control," *Elife*, vol. 10, p. e65878, 2021.
- [40] Q. Xi, Z. Chen, K. Yin, X. Liu, and F. Gao, "Fault-tolerant gait for Hexapod Robots with partial active joints locked," *Mechanism and Machine Theory*, vol. 205, p. 105895, 2025.
- [41] D. Grzelczyk, B. Stanczyk, and J. Awrejcewicz, "Kinematics, dynamics and power consumption analysis of the hexapod robot during walking with tripod gait," *International Journal of Structural Stability and Dynamics*, vol. 17, no. 5, p. 1740010, 2017.
- [42] Y. Zheng, K. Xu, Y. Tian, and X. Ding, "Different manipulation mode analysis of a radial symmetrical hexapod robot with leg—arm integration," *Frontiers of Mechanical Engineering*, vol. 17, no. 1, p. 8, 2022.
- [43] J. Gu, L. Li, S. Zhou, and W. Zhang, "Research on foot trajectory planning of quadruped robot: based on high degree polynomial curve," in *Proceedings of the 2022 4th International Conference on Robotics, Intelligent Control and Artificial Intelligence*, pp. 87-94, 2022.
- [44] P. Ramdya *et al.*, "Climbing favours the tripod gait over alternative faster insect gaits," *Nature communications*, vol. 8, no. 1, p. 14494, 2017.
- [45] T. G. Thuruthel, E. Falotico, M. Manti, and C. Laschi, "Stable Open Loop Control of Soft Robotic Manipulators," in *IEEE Robotics and Automation Letters*, vol. 3, no. 2, pp. 1292-1298, April 2018, doi: 10.1109/LRA.2018.2797241.
- [46] Y. Ding, A. Pandala, C. Li, Y. -H. Shin, and H. -W. Park, "Representation-Free Model Predictive Control for Dynamic Motions in Quadrupeds," in *IEEE Transactions on Robotics*, vol. 37, no. 4, pp. 1154-1171, Aug. 2021, doi: 10.1109/TRO.2020.3046415.
- [47] G. Xin, W. Wolfslag, H.-C. Lin, C. Tiseo, and M. Mistry, "An optimization-based locomotion controller for quadruped robots leveraging cartesian impedance control," *Frontiers in Robotics and AI*, vol. 7, p. 48, 2020.
- [48] G. Picardi, M. Chellapurath, S. Iacoponi, S. Stefanni, C. Laschi, and M. Calisti, "Bioinspired underwater legged robot for seabed exploration with low environmental disturbance," *Science Robotics*, vol. 5, no. 42, 2020.
- [49] Y. Chen, N. Doshi, and R. J. Wood, "Inverted and Inclined Climbing Using Capillary Adhesion in a Quadrupedal Insect-Scale Robot," in *IEEE Robotics and Automation Letters*, vol. 5, no. 3, pp. 4820-4827, July 2020, doi: 10.1109/LRA.2020.3003870.
- [50] X. Meng, S. Wang, Z. Cao, and L. Zhang, "A review of quadruped robots and environment perception," *2016 35th Chinese Control Conference (CCC)*, pp. 6350-6356, 2016, doi: 10.1109/ChiCC.2016.7554355.
- [51] M. Buehler, "Dynamic locomotion with one, four and six-legged robots," *Journal of the Robotics Society of Japan*, vol. 20, no. 3, pp. 237-242, 2002.
- [52] J. Z. Gul, B.-S. Yang, Y. J. Yang, D. E. Chang, and K. H. Choi, "In situ UV curable 3D printing of multi-material tri-legged soft bot with spider mimicked multi-step forward dynamic gait," *Smart Materials and Structures*, vol. 25, no. 11, p. 115009, 2016.
- [53] H. Li and P. M. Wensing, "Hybrid Systems Differential Dynamic Programming for Whole-Body Motion Planning of Legged Robots," in *IEEE Robotics and Automation Letters*, vol. 5, no. 4, pp. 5448-5455, Oct. 2020, doi: 10.1109/LRA.2020.3007475.
- [54] C. Mastalli, I. Havoutis, M. Focchi, D. G. Caldwell, and C. Semini, "Motion Planning for Quadrupedal Locomotion: Coupled Planning, Terrain Mapping, and Whole-Body Control," in *IEEE Transactions on Robotics*, vol. 36, no. 6, pp. 1635-1648, Dec. 2020, doi: 10.1109/TRO.2020.3003464.
- [55] M. Chen, H. Chen, X. Wang, J. X. Yu, and Y. X. Zhang, "Design and control of a novel single leg structure of electrically driven quadruped robot," *Mathematical Problems in Engineering*, vol. 2020, no. 1, pp. 3943867, 2020.
- [56] C. Bal, "Neural coupled central pattern generator based smooth gait transition of a biomimetic hexapod robot," *Neurocomputing*, vol. 420, pp. 210-226, 2021.
- [57] M. Chen, Q. Li, S. Wang, K. Zhang, H. Chen, and Y. Zhang, "Single-leg structural design and foot trajectory planning for a novel bioinspired quadruped robot," *Complexity*, vol. 2021, no. 1, pp. 1-17, Jan. 2021, doi: 10.1155/2021/6627043.
- [58] H. Xia, X. Zhang, and H. Zhang, "A new foot trajectory planning method for legged robots and its application in hexapod robots," *Applied Sciences*, vol. 11, no. 19, p. 9217, 2021.
- [59] Y. Shao, Y. Jin, X. Liu, W. He, H. Wang, and W. Yang, "Learning Free Gait Transition for Quadruped Robots Via Phase-Guided Controller," in *IEEE Robotics and Automation Letters*, vol. 7, no. 2, pp. 1230-1237, April 2022, doi: 10.1109/LRA.2021.3136645.
- [60] Y. K. Kim, W. Seol, and J. Park, "Biomimetic quadruped robot with a spinal joint and optimal spinal motion via reinforcement learning," *Journal of Bionic Engineering*, vol. 18, no. 6, pp. 1280-1290, 2021.

- [61] Y. Ding, A. Pandala, and H. -W. Park, "Real-time Model Predictive Control for Versatile Dynamic Motions in Quadrupedal Robots," *2019 International Conference on Robotics and Automation (ICRA)*, pp. 8484-8490, 2019, doi: 10.1109/ICRA.2019.8793669.
- [62] Y. Yin, F. Gao, Q. Sun, Y. Zhao, and Y. Xiao, "Smart Gait: A Gait Optimization Framework for Hexapod Robots," *Chinese Journal of Mechanical Engineering*, vol. 37, no. 1, p. 15, 2024.
- [63] H. Sun, J. Yang, Y. Jia, and C. Wang, "Free Gait Generation of Quadruped Robots via Impulse-Based Feasibility Analysis," in *IEEE/ASME Transactions on Mechatronics*, vol. 29, no. 1, pp. 412-422, Feb. 2024, doi: 10.1109/TMECH.2023.3279523.
- [64] Z. Qiu, W. Wei, and X. Liu, "Adaptive gait generation for hexapod robots based on reinforcement learning and hierarchical framework," in *Actuators*, vol. 12, no. 2, p. 75, 2023.
- [65] A. Majithia *et al.*, "Design, motions, capabilities, and applications of quadruped robots: a comprehensive review," *Frontiers in Mechanical Engineering*, vol. 10, p. 1448681, 2024.
- [66] J. Ding and Z. Gan, "Breaking Symmetries Leads to Diverse Quadrupedal Gaits," in *IEEE Robotics and Automation Letters*, vol. 9, no. 5, pp. 4782-4789, May 2024, doi: 10.1109/LRA.2024.3384908.
- [67] J. Coelho, B. Dias, G. Lopes, F. Ribeiro, and P. Flores, "Development and implementation of a new approach for posture control of a hexapod robot to walk in irregular terrains," *Robotica*, vol. 42, no. 3, pp. 792-816, 2024.
- [68] C. Bal, "Neural coupled central pattern generator based smooth gait transition of a biomimetic hexapod robot," *Neurocomputing*, vol. 420, pp. 210-226, 2021.
- [69] J. Ma, G. Qiu, W. Guo, P. Li, and G. Ma, "Design, analysis and experiments of hexapod robot with six-link legs for high dynamic locomotion," *Micromachines*, vol. 13, no. 9, p. 1404, 2022.
- [70] N. Mingchinda, V. Jaiton, B. Leung, and P. Manoonpong, "Leg-body coordination strategies for obstacle avoidance and narrow space navigation of multi-segmented, legged robots," *Frontiers in Neurobotics*, vol. 17, p. 1214248, 2023.
- [71] B. Chong *et al.*, "A general locomotion control framework for multi-legged locomotors," *Bioinspiration & Biomimetics*, vol. 17, no. 4, p. 046015, 2022.
- [72] R. Ş. Dologa, H. Vălean, and A. Ianosi, "Design of a Stepping Hexapod Bio-Inspired Robot," *2024 IEEE International Conference on Automation, Quality and Testing, Robotics (AQTR)*, pp. 1-6, 2024, doi: 10.1109/AQTR61889.2024.10554226.
- [73] P. Manoonpong *et al.*, "Insect-inspired robots: bridging biological and artificial systems," *Sensors*, vol. 21, no. 22, p. 7609, 2021.
- [74] J. Comejo *et al.*, "Bio-inspired design of hard-bodied mobile robots based on arthropod morphologies: a 10-year systematic review and bibliometric analysis," *Bioinspiration & Biomimetics*, 2024.
- [75] H. G. Meyer, D. Klimeck, J. Paskarbeit, U. Rückert, M. Egelhaaf, M. Porrman, and A. Schneider, "Resource-efficient bio-inspired visual processing on the hexapod walking robot HECTOR," *Plos one*, vol. 15, no. 4, p. e0230620, 2020.
- [76] Y. Liu, C. Wang, H. Zhang, and J. Zhao, "Research on the posture control method of hexapod robot for rugged terrain," *Applied Sciences*, vol. 10, no. 19, p. 6725, 2020.
- [77] S. Erasmus. *Guidance, control, and motion planning for a hexapod robot moving over uneven terrain*, Doctoral dissertation, Stellenbosch: Stellenbosch University, 2023.
- [78] K. Xu, Y. Lu, L. Shi, J. Li, S. Wang, and T. Lei, "Whole-body stability control with high contact redundancy for wheel-legged hexapod robot driving over rough terrain," *Mechanism and machine theory*, vol. 181, p. 105199, 2023.
- [79] E. A. Parra Ricaurte, J. Pareja, S. Dominguez, and C. Rossi, "Comparison of leg dynamic models for quadrupedal robots with compliant backbone," *Scientific Reports*, vol. 12, no. 1, p. 14579, 2022.
- [80] Y. Liu, X. Fan, L. Ding, J. Wang, T. Liu, and H. Gao, "Fault-tolerant tripod gait planning and verification of a hexapod robot," *Applied Sciences*, vol. 10, no. 8, p. 2959, 2020.